Supplementary Materials

Direct visualization of spin-dependent orbital geometry on the Na_2IrO_3 surface with ultra-high resolution

Xin Zhang[1,#], Zongyuan Zhang[2,#], Jasminka Terzic[3,#], Zhibin Shao[1], Haigen Sun[4], Shaojian Li[4], Krisztián Palotás[5,6], Haoquan Ding[7], Gang Cao[3], Wenliang Zhu[1], Haiping Lin[1], Jianzhi Gao[1], Minghu Pan[1,4]

[1]School of Physics and Information Technology, Shaanxi Normal University, Xi'an 710119, Shannxi, China.

[2]Information Materials and Intelligent Sensing Laboratory of Anhui Province, Institutes of Physical Science and Information Technology, Anhui University, Hefei 230601, Anhui, China

[3]Department of Physics, University of Colorado at Boulder, Boulder, CO 80309, USA.

[4]School of Physics, Huazhong University of Science and Technology, Wuhan 430074, Hubei, China.

[5]Wigner Research Center for Physics, Budapest H-1525, Hungary.

[6]MTA-SZTE Reaction Kinetics and Surface Chemistry Research Group, University of Szeged, Szeged H-6720, Hungary.

[7]School of Physics and Astronomy, University of Birmingham, Birmingham B15 2TT, UK.

#Authors contributed equally.

1. Methods

STM: The cleaved sample was quickly transferred into a Unisoko-1300 commercial STM for measurement at a temperature of 77 K. A commercial Pt-Ir tip was prepared by gentle field emission above a clean Au(111) sample. The bias voltage was applied on the sample during the STM observations. The STM images were analyzed using WSxM (*36*). The resistivity of the samples increases dramatically upon further cooling (*10*), which prevents us to conduct the STM/S measurements at temperatures much lower than 77 K.

Preparation of O-decorated tip: By applying a voltage pulse of −3 V with time duration about 100 ms on the Na_2IrO_3 sample so that the voltage pulse can excite and break Na-O bond, the oxygen anion will be released and attracted to the positive bias on the tip. Such procedure is performed in ultrahigh vacuum and at room temperature. A monitor is used for monitoring the variation of tunneling current. Before functionalizing the tip with surface oxygen, a clean metal tip need be preheated by a tungsten wire ring with apply a current about 2 A in order to remove the oxide layer at the apex of tip.

Sample preparation: A self-flux method was used to grow the Na_2IrO_3 single crystals from off-stoichiometric quantities of IrO_2 and Na_2CO_3. The preparation details can be found elsewhere (*10, 14, 51-53*). The crystals used in this study have the typical sizes of 2 mm × 2 mm × 0.5 mm. Samples were cleaved *in situ* at room temperature (RT) under vacuum with pressure better than 1×10^{-10} torr, resulting in shiny surfaces.

Calculation: The first-principles DFT calculations were carried out with the Vienna Ab Initio Simulation Package (VASP) (*37*). The core and valence electronic interactions were described with the frozen-core projector augmented-wave (PAW) potentials (*38*). The Kohn-Sham single electron states were expanded in plane waves with a kinetic energy of up to 400 eV. The exchange correlation energy was calculated with the Perdew-Burke-Ernzerhof (PBE) of generalized gradient approximation (GGA) (*39*). The tolerance of 10^{-4} eV was chosen for energy convergence of electronic calculations. The Na_2IrO_3 was modelled with a (2×2) unit cell. The metal STM tip was modelled with a pyramid of Ir(111) in which the apex is a single Ir atom. The oxygen functionalized tip was mimicked by an Ir(111) pyramid with five oxygen atoms at the apex. A large vacuum of 25 Å along the direction normal to the surface was employed to separate surfaces from their periodic images. The Brillouin zone of

reciprocal space was modeled based on the Γ centered Monkhorst-Pack scheme, where a 4×2×1 gird was adopted in geometry optimizations, searches of the transition states and calculations of electronic properties. STM images were simulated using the revised Chen method implemented in the bSKAN code (*40*).

2. Optimized surface structure of Na_2IrO_3

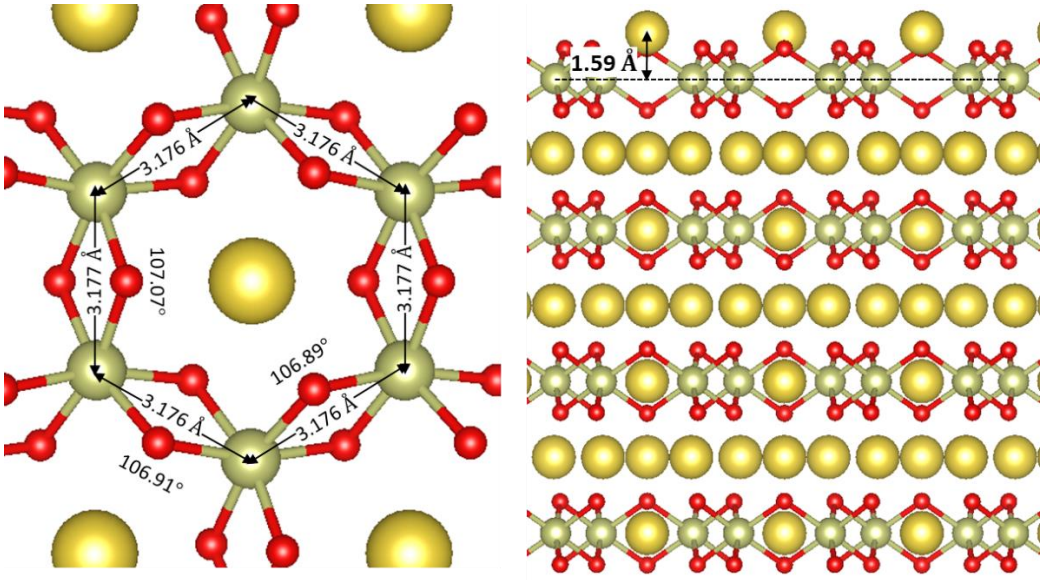

Fig S1. Top view (left) and side view (right) of the optimized Na_2IrO_3 surface.

3. *In situ* annealing of the samples

According to the previous work (*54*), the strongly bonded IrO_6 octahedra can keep intact during the cleaving process, while the pure Na layer and the Na atoms in the $NaIr_2O_6$ layer are volatile. In present work, a dominating 1×1 periodic Na surface (Fig. S1A) is obtained after the cleaving process except for a number of atomic defects (see Fig. 1B for details). In order to tune the content of the surface Na atoms, we annealed the sample at 300 °C for 5 min. As shown in Supplementary Fig. 1B, a $(\sqrt{3}\times\sqrt{3})R30°$ unit cell is identified. Hence, This $(\sqrt{3}\times\sqrt{3})R30°$ surface is consistent with previous reports (*51*), where two-thirds of the Na atoms are removed out of the surface $NaIr_2O_6$ layer during the annealing. In addition, more bright spots are found after annealing, which can be sort as oxygen vacancies (see the main text of this paper).

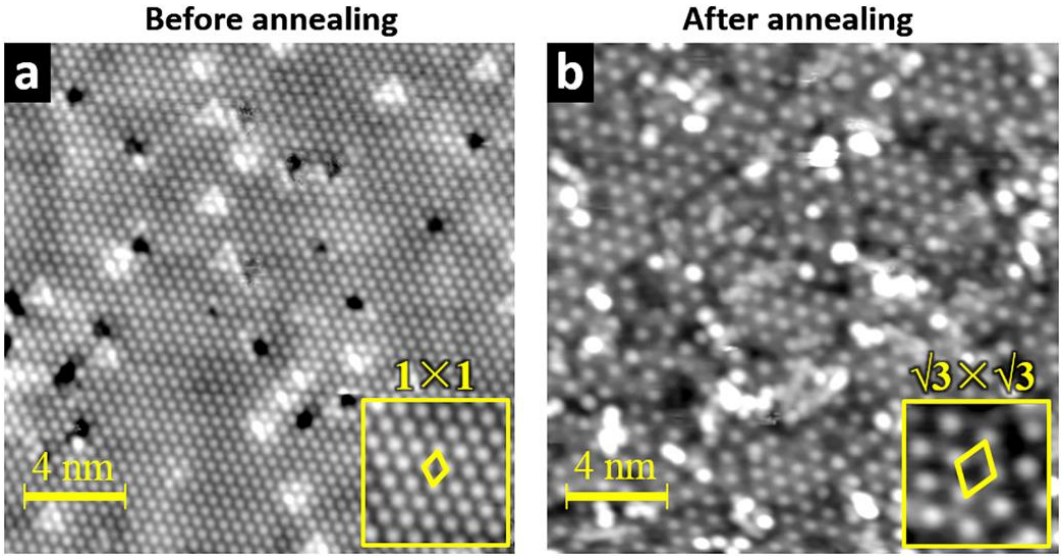

Fig. S2. STM topographic images measured before (**A**) and after (**B**) annealing (V_b = +2 V, I_t = 20 pA, image size: 20 × 20 nm^2). The insets of (**A**) and (**B**) are the corresponding zoomed images. The yellow rhombus in the insets represent the 1×1 and (√3×√3)*R*30° unit cell, respectively.

We measured the d*I*/d*V* spectra on the surfaces before and after annealing (Supplementary Fig. S2). The insulating gap of the annealed surface is 300 meV, which is 120 meV narrower than that measured on the pristine one (420 meV). In addition, there is a small shift of the gap feature in the spectra, implying an electron doping during the annealing. In conclusion, both the surface morphologies and electronic properties can be tuned by the simple annealing, which provides a strategy for studying the lattice structure and doping characteristics of the A_2IrO_3 materials.

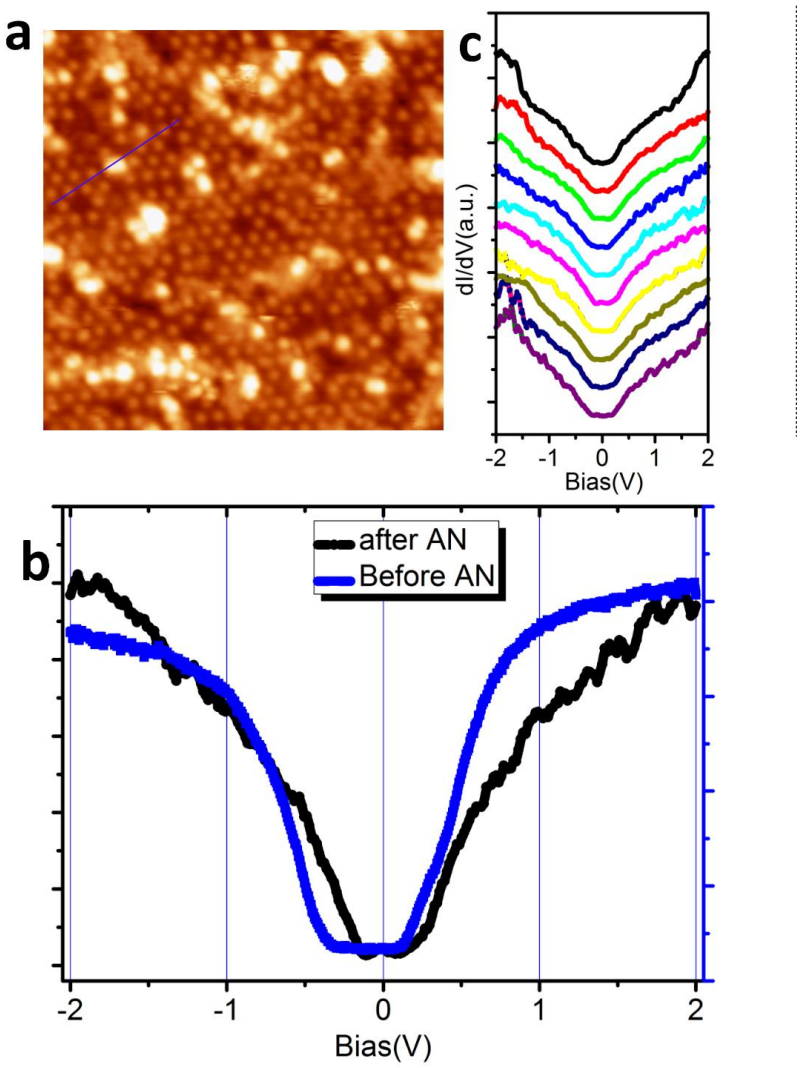

Fig. S3. Topographic image and d*I*/d*V* spectra taken on the samples after *in situ* annealing. (**A**) Topographic image after annealing at 300 °C for 5 min. (V_b = −2.0 V, I_t = 50 pA, image size: 20 × 20 nm^2). (**B**) d*I*/d*V* spectra measured before and after annealing. (**C**) Spectra measured along the line marked in (**A**). The spectra across these bright spots shows similar gap features. d*I*/d*V* spectra were acquired using a lock-in technique with *ac* modulation of 10 mV.

4. Optimized surface structure of Na_2IrO_3

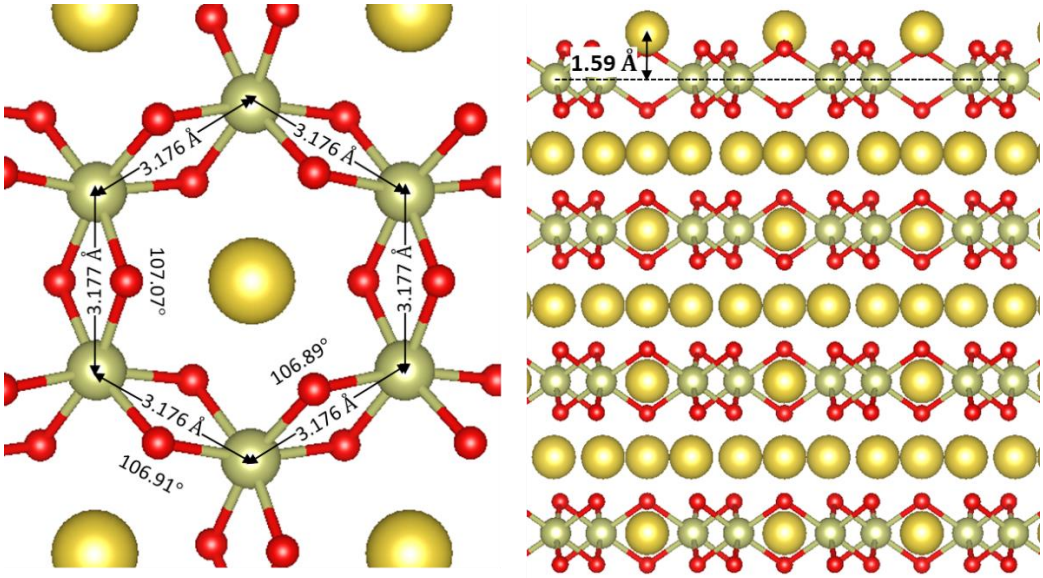

Fig S3. Top view (left) and side view (right) of the optimized Na_2IrO_3 surface.

5. Functionalizing the STM tip with surface oxygen

By applying a voltage pulse of −3 V on the sample so that the voltage pulse can excite and break Na-O bond and the oxygen anion will be released and attracted to the positive bias on the tip . The process would create an oxygen vacancy on the surface, which can be visualized by the successive images (Fig. S4B). In addition, one can immediately notice from Fig. S4B that the resolution became better once the tip is decorated with oxygen atoms.

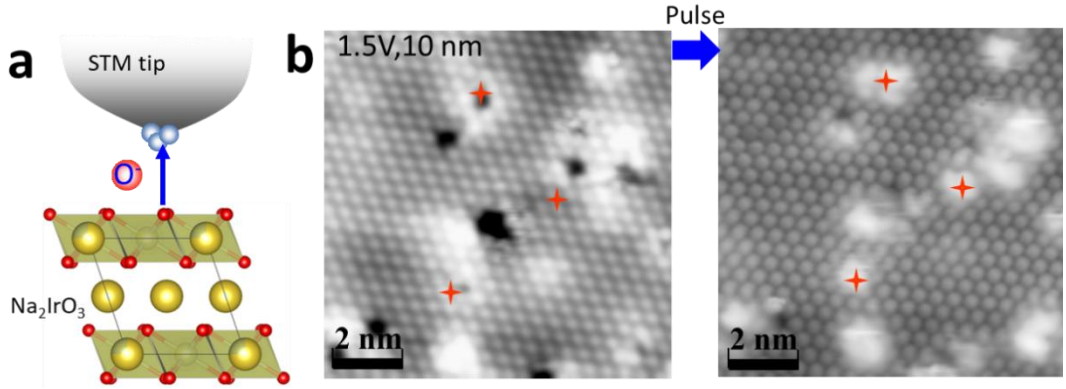

Fig. S4. Preparation of the O-decorated STM tip. (**A**) Schematic drawings illustrate the methodology to prepare the O-decorated tip. (**B**) Two STM images in successive scan at the same location. (left) the initial image; (right) the image showing the newly emerged, three O vacancies (marked as red stars) after applying the pulses, taken by O-decorated tip.

6. Bias dependent STM images with an O-tip

With an O decorated tip, The STM images vary with the sample biases. At -1.8 V, the entire surface exhibits a hexagonal lattice (Fig. S5A). At -1.6 V to -1.2 V, however, anisotropic pattern is observed at the regions that are away from the oxygen vacancies, while the hexagonal lattice maintains at the region adjacent to the oxygen vacancies, as shown in Fig. S5B.

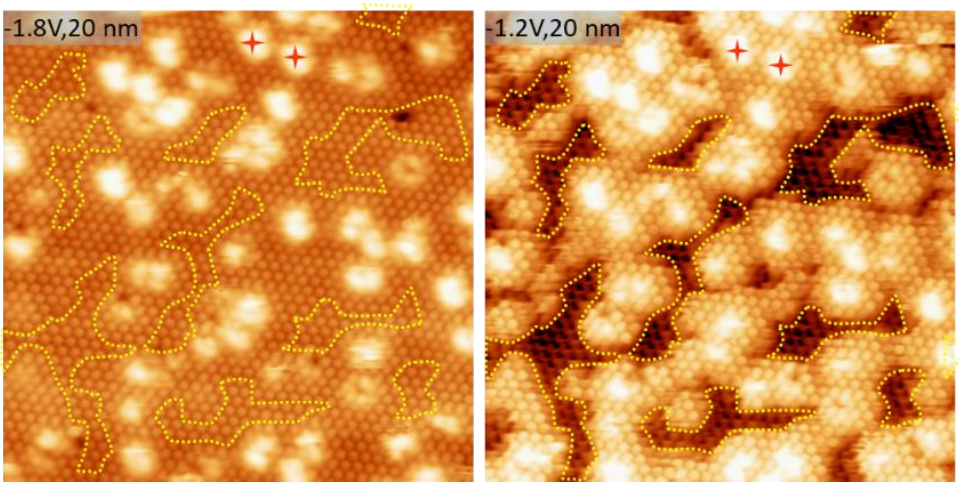

Fig. S5. Bias dependent STM images with an O-terminated tip. The bias voltage is -1.8 V for (**A**) and -1.2 V for (**B**). The tunneling current is 20 pA and the image size is 20 × 20 nm^2 for both figures.

References and Notes

51. S. Chikara *et al.*, Giant magnetoelectric effect in the J_{eff} = 1/2 Mott insulator Sr_2IrO_4. *Phys. Rev. B* **80**, 140407 (2009). DOI: 10.1103/PhysRevB.80.140407.

52. M. A. Laguna-Marco *et al.*, Orbital magnetism and spin-orbit effects in the electronic structure of $BaIrO_3$. *Phys. Rev. Lett.* **105**, 216407 (2010). DOI: 10.1103/PhysRevLett.105.216407.

53. M. Ge *et al.*, Lattice-driven magnetoresistivity and metal-insulator transition in single-layered iridates. *Phys. Rev. B* **84**, 100402 (2011). DOI: 10.1103/PhysRevB.84.100402.

54. F. Lüpke et al., Highly unconventional surface reconstruction of Na_2IrO_3 with persistent energy gap. *Phys. Rev. B* **91**, 041405 (2015). DOI:10.1103/PhysRevB.91.041405.